Contribution from the Departments of Chemistry, The University of North Carolina at Chapel Hill, Chapel Hill, North Carolina 27514, The University of Arkansas, Fayetteville, Arkansas 72701, and The University of North Carolina at Charlotte, Charlotte, North Carolina 28223

Excited-State Photoelectrochemical Cells for the Generation of H_2 and O_2 Based on $Ru(bpy)_3^{2+}$*

WALTER J. DRESSICK, THOMAS J. MEYER,* BILL DURHAM, and D. PAUL RILLEMA

Received November 6, 1981

Excited-state photoelectrochemical cells are described for the production of H_2 or O_2 (or I_2) in aqueous solution. The cells are based on visible excitation of $Ru(bpy)_3^{2+}$ followed by oxidative quenching of the resulting charge-transfer excited state(s). In the H_2 cell, the quencher is paraquat (PQ^{2+}, 1,1′-Me_2-4,4′-bpy^{2+}), and back electron transfer between $Ru(bpy)_3^{3+}$ and PQ^+ is inhibited by the addition of the reductive scavengers triethanolamine, cysteine, or sodium ethylenediaminetetraacetate, which rapidly reduce $Ru(bpy)_3^{3+}$ to $Ru(bpy)_3^{2+}$. The result is to build up PQ^+ in the photolysis cell, which is used to reduce H^+ to H_2 in a separate cell compartment, at a platinum electrode. In the O_2 (or I_2) cell, $Co^{III}(C_2O_4)_3^{3-}$ ($C_2O_4^{2-}$ is oxalate) acts as quencher. Reduction to Co(II) results in rapid aquation to give $Co^{2+}(aq)$, and a back-electron-transfer reaction involving $Ru(bpy)_3^{3+}$ is avoided. Visible photolysis leads to the production of $Ru(bpy)_3^{3+}$, which is then used to oxidize OH^- to O_2 (or I^- to I_3^-) in a second cell compartment. Variations in photocurrents in the cells as a function of such variables as pH, quencher concentration, and scavenger concentration are in good agreement with the predictions of a theoretical model developed earlier for a related cell.

Introduction

A theme that continues to evolve in photochemistry is the use of molecular excited states in energy conversion schemes based on the production of either electrical or stored chemical energy. The photodecomposition of H_2O into H_2 and O_2 using visible light is an especially attractive possibility, and the results of a number of experiments related to this objective have been published.[1,2] As described here and in earlier publications,[3,4] one approach to the problem is photoelectrochemical in nature, based on the initial electron-transfer quenching of molecular excited states. In contrast to more conventional photoelectrochemical cells (PEC) where charge separation and a photopotential are created by light absorption at a semiconductor/solution interface,[5] in excited-state PEC cells, light absorption leads to a molecular excited state, which subsequently undergoes electron-transfer quenching. The electrode functions only as a collector of redox products produced by photolysis in the solution and as a means for transferring electrons to or from a second cell compartment. There are both clear advantages and disadvantages associated with such cells. The intent of this paper is to describe two cells, one for the photoproduction of H_2 and one for the photoproduction of O_2, and to discuss some general features of the excited-state PEC experiment.

Experimental Section

Materials. The salts $[Ru(bpy)_3]Cl_2$ (bpy is 2,2′-bipyridine), $[Ru(phen)_3]Cl_2$ (phen is 1,10-phenanthroline),[6] and $K_3Co(Ox)_3$ (Ox is oxalate, $C_2O_4^{2-}$)[7] were prepared and purified as described in the literature. Sulfuric acid, Na_2SO_4, NaCl, $NaClO_4$, KI, oxalic acid, NaOH, sodium borate, HCl, agar, and potassium hydrogen phosphate were all Fisher ACS grade and were used as received. Triethanolamine (TEOA) from Aldrich was used as received. Sodium ethylenediaminetetraacetate (Na_4EDTA) was obtained from Fisher and recrystallized once from H_2O prior to use. Cysteine hydrochloride from Aldrich was recrystallized twice from ethanol immediately prior to use. Methylviologen dichloride

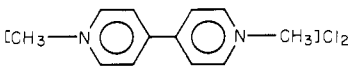

($[PQ]Cl_2$) was obtained from Aldrich and recrystallized once from H_2O before use. PbO_2 (Alfa Ventron) was used as received.

Solutions for the PEC experiments were prepared with use of conductivity H_2O (17-MΩ resistance). The saturated KCl/agar salt bridges were prepared by literature methods.[8] Such bridges normally had a resistance of approximately 1000 Ω. Since the salt bridge resistance comprises the major fraction of the cell resistance and because the external resistor (1000 Ω) is nearly equal to the internal cell resistance, the cells were operating at maximum power output during the experiments. The anode solutions were Ar bubble degassed for 20 min prior to the beginning of each expeiment for all cells. Degassing was not necessary for the $Ru(bpy)_3^{3+}$/oxalic acid kinetic study.

Photolyses. The photoelectrochemical cell and photolysis apparatus used in our experiments were described previously.[9] In all experiments, 436-nm light was used. The output light from the monochromator was allowed to strike the face of the anode (H_2 cell) or cathode (O_2 cell) half-cell on which a Pt-screen electrode was mounted. The light intensity at the excitation wavelength of 436 nm was $(2.88 \pm 0.15) \times 10^{-8}$ einstein/s as determined by Reinecke's salt actinometry.[10] All components including the cell were mounted on an optical bench for stability.

The photocurrents generated in the operation of the cells were measured by dropping their outputs across a 1000-Ω (1%) resistor. The voltage drop across the resistor was monitored with a Hew-

* To whom correspondence should be addressed at The University of North Carolina at Chapel Hill.

(1) Examples of H_2-producing systems include: (a) Kalyanosundaran, K.; Kiwi, J.; Grätzel, M. *Helv. Chim. Acta* **1978**, *61*, 2720. (b) DeLaive, P. J.; Sullivan, B. P.; Meyer, T. J.; Whitten, D. G. *J. Am. Chem. Soc.* **1979**, *101*, 4007. (c) Kawai, T.; Tanimura, K.; Sakada, T. *Chem. Lett.* **1979**, 137. (d) Kirsch, M.; Lehn, J. M.; Sauvage, J. P. *Helv. Chim. Acta* **1979**, *62*, 1345. (e) Kiwi, J.; Graätzel, M. *Nature (London)* **1979**, *281*, 657.

(2) Some O_2-producing systems include: (a) Kiwi, J.; Grätzel, M. *Angew. Chem., Int. Ed. Engl.* **1978**, *17*, 860. (b) Lehn, J. M.; Sauvage, J. P.; Ziessel, R. *Nouv. J. Chim.* **1979**, *3*, 423. (c) Kiwi, J.; Grätzel, M. *Angew. Chem.* **1979**, *91*, 659. (d) Kalyanasundaran, K.; Micic, O.; Promauro, E.; Grätzel, M. *Helv. Chim. Acta* **1979**, *62*, 2432. (e) Neumann-Spallert, M.; Kalyanasundaran, K. *J. Chem. Soc., Chem. Commun.* **1981**, 437.

(3) (a) Durham, B.; Dressick, W. J.; Meyer, T. J. *J. Chem. Soc., Chem. Commun.* **1979**, 381. (b) Rillema, D. P.; Dressick, W. J.; Meyer, T. J. *Ibid.* **1980**, 247.

(4) (a) Neumann-Spallart, M.; Kalayanasundara, K. *Ber. Bunsenges. Phys. Chem.* **1981**, *85*, 704. (b) Humphry-Baker, R.; Lilie, J.; Grätzel, M. *J. Am. Chem. Soc.* **1982**, *104*, 427.

(5) For a general survey of semiconductors as applied to this problem, see the following: (a) Wrighton, M. *Acc. Chem. Res.* **1979**, *12*, 303. (b) Nozik, A. *Annu. Rev. Phys. Chem.* **1978**, *29*, 189.

(6) Braddock, J. N.; Meyer, T. J. *J. Am. Chem. Soc.* **1973**, *95*, 3158.

(7) Palmer, W. G. "Experimental Inorganic Chemistry"; Cambridge University Press: New York, 1954; pp 550–554.

(8) Meites, L. "Polarographic Techniques"; Interscience: New York, 1965; p 63.

(9) Dressick, W. J.; Meyer, T. J.; Durham, B. *Isr. J. Chem.*, in press. Dressick, W. J. Ph.D. Thesis, The University of North Carolina, Chapel Hill, NC, 1981.

(10) Wegner, E. E.; Adamson, A. W. *J. Am. Chem. Soc.* **1966**, *88*, 394.

0020-1669/82/1321-3451$01.25/0

lett-Packard 7004B X-Y recorder equipped with a 17172A time base and 17171A dc preamplifier. Photopotentials and pH measurements were made with a Radiometer PHM62 pH meter with a Model G202C pH electrode and Model K401 saturated calomel reference electrode. The cell was not thermostated since temperature variations did not exceed 1 °C. Oxygen in the Ar streams used for degassing was removed by passage of the gas stream through a 30 × 4 cm diameter column of BTS R311 CuO catalyst, which had been activated with H_2 for 24 h prior to use.

Photoelectrochemical Experiments. Experiments involving photoelectrochemical cells were carried out as follows. All manipulations were carried out in the dark. For the O_2 or I_2 cells, the anode was first charged with the appropriate solution (NaOH in 1.0 M Na_2SO_4 for the O_2 cell and 1.0 M KI in 1.0 M $NaClO_4$ or 1.0 M H_2SO_4 for the I_2 cell) and the agar salt bridge placed in the solution. The aqueous anode solution was Ar bubble degassed for 20 min. A solution containing $[Ru(bpy)_3]Cl_2$ and $K_3[Co(Ox)_3]$ in 1.0 M H_2SO_4 was prepared and placed in the photocathode compartment. The remaining arm of the salt bridge was placed in contact with this solution, and the output of the cell dropped across the 1000-Ω resistor. The anode was a 1 × 1 cm Pt-foil electrode. The recorder used to measure the photocurrents and the stirring system were activated, and the dark-current base line was allowed to stabilize (~5 min). The stirring system used and the associated calibration technique for determining stirring rate have been described previously.[9] For the initiation of a run, the shutter of the Xe lamp was opened and the photocurrent was plotted as a function of time. The system usually required 3–4 min to reach a steady state. At the conclusion of the experiment, the lamp was extinguished and the current allowed to decay to the initial dark value. In those cases where open-circuit photopotentials were measured, the 1000-Ω resistor was simply replaced by the Radiometer pH meter.

The I_2 produced in the I_2 cell was determined spectrophotometrically in H_2O as the I_3^- ion. The absorbance maximum of I_3^- at 352 nm in H_2O was monitored with a Bausch and Lomb Model 210 UV spectrophotometer. Solution blanks were prepared in a manner identical with that for the anode cell solutions and stored in the dark. A calibration curve was prepared and found to be linear for $[I_2] \leq 5 \times 10^{-4}$ M in 1.0 M I^-.

The procedure for the H_2 cell was essentially the same as that just described for the O_2 cell. In this case, however, the photoanode was charged with the appropriate solutions containing $[Ru(bpy)_3]Cl_2$, $[PQ]Cl_2$, and scavenger (TEOA, $EDTA^{4-}$, or cysteine) and degassed as before. The central compartment of the cell contained a saturated sodium borate buffer in 0.1 M NaCl solution, which replaced the agar salt bridge used in the O_2 cell. The cathode solution contained 1.0 M HCl. The cathode was a 1 × 1 cm platinized Pt-foil electrode. For the H_2 generation experiments, the cathode compartment was also degassed with Ar. The remainder of the procedure was identical with that for the O_2 experiments.

Analysis of the H_2 or O_2 produced was determined by gas chromatography. A neutral 10 ft × $^1/_8$ in. diameter alumina column operated at the temperature of a dry ice/ethanol bath with Ar carrier gas was utilized.

In all of the photoelectrochemical experiments described here the observed output of the cells was determined by the characteristics of the photoelectrode. Variations in the dark electrode in such quantities as pH or $[I^-]$ in the range used here had *no* effect on the observed photocurrent response of the cells.

Kinetics of the Oxidation of Oxalic Acid by $Ru(bpy)_3^{3+}$. The kinetics of the reaction between $Ru(bpy)_3^{3+}$ and oxalic acid were studied with a Gilford Model 240 spectrophotometer and an Aminco Model 4-8409 stopped-flow system described previously.[11] Signals were recovered with a Biomation Model 1010 wave form recorder in conjunction with the Hewlett-Packard recorder mentioned previously. The system was thermostated with a Forma Scientific Model 2095 constant-temperature bath. The temperatures were found to be stable within ±0.1 °C for each experiment.

In a typical experiment, $Ru(bpy)_3^{3+}$ was generated from a solution of $[Ru(bpy)_3]Cl_2$ (with $[Na_2SO_4] + [H_2SO_4] = 1.0$ M) by the addition of PbO_2. The filtered Ru^{III} solution was allowed to equilibrate for 20 min in the temperature bath prior to the addition of the equilibrated oxalic acid solution (with $[Na_2SO_4] + [H_2SO_4] = 1.0$ M) to initiate the reaction. The rate of regeneration of $Ru(bpy)_3^{2+}$ was followed by monitoring the absorbance increase at $\lambda = 453$ nm. Rate constants were obtained as the slopes of plots of ln (absorbance) vs. time, which were found to be linear over 3–4 half-lives. The identification of CO_2 as the oxidation product of the oxalic acid and the determination of the reaction stoichiometry were accomplished by mixing equal volumes of 10^{-3} M $Ru(bpy)_3^{3+}$ and saturated oxalic acid in a cuvette flushed with Ar and capped with a rubber septum. At the conclusion of the reaction, a sample of the atmosphere was injected into the gas chromatograph, which was also used for the detection of H_2 and O_2 as described above. The CO_2 was identified by its retention time, and the stoichiometry was determined with the aid of a CO_2 calibration curve.

Results and Discussion

The bases for both of the excited-state PEC systems described here are the same. They involve optical excitation of a molecular excited state followed by one-electron-transfer quenching using either an oxidizing or a reducing quencher. The excited state used here is the emitting metal-to-ligand charge-transfer (MLCT) excited state(s) of $Ru(bpy)_3^{2+}$ (bpy is 2,2′-bipyridine), $Ru(bpy)_3^{2+*}$. The photochemical[12] and photophysical[13] properties of the excited state have been studied. It has well-defined redox properties as both an oxidant and a reductant[14] and is sufficiently long-lived (600 ns in deaerated aqueous solution at room temperature) to undergo bimolecular electron transfer.

The redox properties of the excited state provide a basis in chemical reactivity for coupling the energy stored in the excited state with the external environment. Following optical excitation, which is a light to excited-state energy conversion step, eq 1, electron-transfer quenching either oxidatively or re-

$$Ru(bpy)_3^{2+} \xrightarrow{h\nu} Ru(bpy)_3^{2+*} \quad (1)$$

ductively,[15] e.g., eq 2 (PQ^{2+} is 1,1′-Me_2-4,4′-bpy^{2+}), results

$$Ru(bpy)_3^{2+*} + PQ^{2+} \rightarrow Ru(bpy)_3^{3+} + PQ^{+} \quad (2)$$

in the conversion of excited-state energy to stored chemical redox energy. The redox energy is stored transiently because of back electron transfer (eq 3). The result of eq 2 is to

$$Ru(bpy)_3^{3+} + PQ^{+} \rightarrow Ru(bpy)_3^{2+} + PQ^{2+} \quad (3)$$

produce an oxidant ($Ru(bpy)_3^{3+}$) thermodynamically capable of oxidizing water to O_2 ($E^{\circ\prime}$ = 1.26 V vs. NHE) and a reductant (PQ^+) thermodynamically capable of reducing water to H_2 over a broad pH region ($E^{\circ\prime} = -0.46$ V).[17] If one of the quenching products is scavenged, back electron transfer can be avoided and either the oxidation or reduction of water studied separately.

Such schemes provide the basis for the excited-state PEC cells described here. If the first, Scheme I, $Ru(bpy)_3^{3+}$ produced by oxidative quenching is scavenged by a reductant S_{red} (EDTA, cysteine, or triethanolamine), which undergoes an irreversible one-electron oxidation.[16] For the amines the net oxidation involves a two-electron oxidation to give amine and aldehyde products.[16b] The result is to build up the reductant

(11) Cramer, J. L. Ph.D. Dissertation, The University of North Carolina, Chapel Hill, NC, 1974.

(12) Van Houten, T.; Watts, R. J. *Inorg. Chem.* **1978**, *17*, 3381. Durham, B.; Caspar, J. V.; Nagle, J. K.; Meyer, T. J. *J. Am. Chem. Soc.*, in press.

(13) Hipps, K. W.; Crosby, G. A. *J. Am. Chem. Soc.* **1975**, *97*, 7042. Felix, F.; Ferguson, J.; Gudel, H. U.; Ludi, A. *Ibid.* **1980**, *102*, 4096, 4102.

(14) Bock, C. R.; Connor, J. A.; Gutierrez, A. R.; Meyer, T. J.; Whitten, D. G.; Sullivan, B. P.; Nagle, J. K. *J. Am. Chem. Soc.* **1979**, *101*, 4815–4824.

(15) (a) Bock, C. R.; Meyer, T. J.; Whitten, D. G. *J. Am. Chem. Soc.* **1974**, *96*, 4710. (b) Maestri, M.; Grätzel, M. *Ber. Bunsenges. Phys. Chem.* **1977**, *81*, 504. Anderson, C. P.; Salmon, D. J.; Meyer, T. J. *J. Am. Chem. Soc.* **1977**, *99*, 1980. (c) Kalayanasundaran, K.; Kiwi, J.; Grätzel, M. *Helv. Chim. Acta* **1978**, *61*, 2720.

(16) (a) Krasna, A. I. *Photochem. Photobiol.* **1979**, *29*, 267. (b) Smith, P. J.; Mann, C. K. *J. Org. Chem.* **1969**, *34*, 1821 (and references therein).

(17) Curtis, J. C.; Sullivan, B. P.; Meyer, T. J. *Inorg. Chem.* **1980**, *19*, 3833.

PQ^+ in the photocompartment of an electrochemical cell, which is then used to generate H_2 in a second cell compartment (eq 7 and 8). The net reaction in the cell becomes the photochemically induced reduction of water and oxidation of S

$$S_{red} + 2H^+ + 2h\nu \rightarrow S_{ox} + H_2$$

rather than water splitting, where water is both oxidized and reduced. However, such studies are of value in the ultimate design of related systems where water splitting or other light to chemical energy conversion schemes may become a reality.

Scheme I

Photoanode

$$Ru(bpy)_3^{2+} \xrightarrow{h\nu} Ru(bpy)_3^{2+*} \quad (1)$$

$$Ru(bpy)_3^{2+*} + PQ^{2+} \rightarrow Ru(bpy)_3^{3+} + PQ^+ \quad (4)$$

$$Ru(bpy)_3^{3+} + PQ^+ \rightarrow Ru(bpy)_3^{2+} + PQ^{2+} \quad (5)$$

$$S + Ru(bpy)_3^{3+} \rightarrow Ru(bpy)_3^{2+} + S_{ox} \quad (6)$$

$$PQ^+ \xrightarrow{Pt} PQ^{2+} + e^- \quad (7)$$

Cathode

$$H^+ + e^- \xrightarrow{Pt} {}^1/_2H_2 \quad (8)$$

The approach we have taken for oxygen production is a variation on the same theme. Here, as shown in Scheme II, oxidative quenching also occurs, but now, as in the work of Gafney and Adamson[18] and of Demas and Adamson,[19] the quencher $Co(Ox)_3^{3-}$ (Ox is oxalate, $C_2O_4^{2-}$) is reduced and undergoes an irreversible chemical change in aqueous solution to give $Co(H_2O)_6^{2+}$. A back electron transfer is avoided because $Ru(bpy)_3^{3+}$ is insufficiently powerful as an oxidant to oxidize Co^{2+} to Co^{3+} ($E_{1/2}(Co^{3+/2+}) \simeq 1.84$ V. in 3 M HNO_3 vs. NHE)[20] in aqueous solution. Rather, water oxidation occurs in a second cell compartment, again by electron transfer through the external circuit but now in the sense opposite from the H_2 cell.

Scheme II

Photocathode

$$Ru(bpy)_3^{2+} \xrightarrow{h\nu} Ru(bpy)_3^{2+*} \quad (1)$$

$$Ru(bpy)_3^{2+*} + Co(Ox)_3^{3-} \rightarrow Ru(bpy)_3^{3+} + Co(Ox)_3^{4-} \quad (9)$$

$$6H_3O^+ + Co(Ox)_3^{4-} \xrightarrow{fast} Co(H_2O)_6^{2+} + 3H_2(Ox) \quad (10)$$

$$Ru(bpy)_3^{3+} + e^- \xrightarrow{Pt} Ru(bpy)_3^{2+} \quad (11)$$

Anode

$$OH^- \xrightarrow{Pt} {}^1/_4O_2 + {}^1/_2H_2O + e^- \quad (12)$$

A theoretical treatment has been developed that describes the photocharge and photocurrent characteristics of cells like those described in Schemes I and II.[9] The cells are operated under conditions where the observed photocurrents are limited by the current characteristics of the photocompartment. Under these conditions and with a kinetic analysis based on excitation, followed by irreversible quenching, the *total* charge transferred through the cell resulting from photolysis is given by eq 13.

$$q = nFI^0_\lambda 10^{-A_s}(1 - 10^{-(A_{Ru}+A_Q)})\frac{A_{Ru}}{A_{Ru} + A_Q}\phi_1\phi_2\phi_3 t \quad (13)$$

Equation 13 is derived with the assumption that no back electron transfer occurs between the separated redox products, where q is the total charge transferred arising from both light and dark currents, n is the number of electrons transferred in the photo-half-cell, with $n = 1$ for both cells described here, where the electron-transfer carriers are PQ^+ or $Ru(bpy)_3^{3+}$, F is the Faraday constant, 96 496 C/equiv, I^0_λ is the incident light intensity at wavelength λ, A_s is the absorbance of the platinum-screen collector electrode in the photo-half-cell, A_{Ru} is the absorbance of $Ru(bpy)_3^{2+}$ at λ, A_Q is the absorbance of the quencher, Q, at λ, t is the photolysis time, ϕ_1 is the efficiency of formation of the MLCT excited state following excitation, with $\phi_1 = 1$ for $Ru(bpy)_3^{2+}$,[21] ϕ_2 is the quenching efficiency, $\phi_2 = K_{sv}[Q]/(1 + K_{sv}[Q])$, where K_{sv}, the Stern–Volmer constant, is the product of the quenching rate constant, k_q (note eq 4 and 9), and the excited-state lifetime, τ_0, with τ_0 being 600 ± 20 ns in deaerated aqueous solution at room temperature, and ϕ_3 is the separation efficiency following electron transfer where the competition is between redox product separation (k) and back electron transfer before separation (k') with the assumption that quenching is solely by electron transfer:

$$Ru(bpy)_3^{2+}{}_*,\ PQ^{2+} \longrightarrow Ru(bpy)_3^{3+},\ PQ^+$$

$$\swarrow^{k} \qquad \searrow^{k'}$$

$$Ru(bpy)_3^{3+} + PQ^+ \qquad Ru(bpy)_3^{2+},\ PQ^{2+}$$

$$\phi_3 = k/(k + k')$$

For monochromatic irradiation the operating efficiency of the cell, in moles of unit electron charge produced in the cell per einstein entering the cell, is given by eq 14a and the intrinsic efficiency of the cell, in moles of charge per einstein absorbed, is given by eq 14b. The maximum or theoretical

$$\phi_{cell} = 10^{-A_s}(1 - 10^{-(A_{Ru}+A_Q)})\frac{A_{Ru}}{A_{Ru} + A_Q}\phi_1\phi_2\phi_3 = \frac{q}{nFI^0_\lambda t} \quad (14a)$$

$$\Phi_{intrinsic} = \phi_1\phi_2\phi_3 \quad (14b)$$

per photon efficiency of such a cell where the quencher concentration is sufficiently high that $\phi_2 = 1$ is given by the product $\phi_1\phi_3 = \Phi_{max}$, or since $\phi_1 \approx 1$,[21] Φ_{max} is equal to the redox product separation yield, eq 15. The maximum efficiency can be reached under conditions where the collector electrode is removed from the light path ($A_s = 0$), the sensitizer concentration is high, $1 - 10^{-A_{Ru}} \approx 1$, the quencher is not a competitive light absorber ($A_{Ru} >> A_Q$), and the quencher concentration is high ($\phi_2 \rightarrow 1$). Although our experiments were carried out with use of monochromatic irradiation (436 nm), it should be noted that $Ru(bpy)_3^{2+}$ and related complexes are broad-band absorbers in the visible region. Earlier work has shown[3,4,9] that the wavelength dependence of Φ_{cell} arises from the absorbance term in eq 14a. The absorbance term contains contributions from both the sensitizer, A_{Ru} and quencher, A_Q. In general, a contribution to the total absorbance can exist from the photoredox products as well. For example, in the H_2 cell the photogenerated PQ^+ radical absorbs strongly at 436 nm ($\epsilon \sim 2 \times 10^3$ M^{-1} cm^{-1}). In our experiments, inner filter effects from photoredox products are neg-

$$\Phi_{max} = \phi_3 \quad (15)$$

(18) Gafney, H. D.; Adamson, A. W. *J. Am. Chem. Soc.* **1972**, *94*, 8238.
(19) Demas, J. N.; Adamson, A. W. *J. Am. Chem. Soc.* **1973**, *95*, 5159.
(20) Latimer, W. M. "Oxidation Potentials", 2nd ed.; Prentice-Hall: Englewood Cliffs, NJ; p 213.
(21) Demas, J. N.; Taylor, D. G. *Inorg. Chem.* **1979**, *18*, 3177.

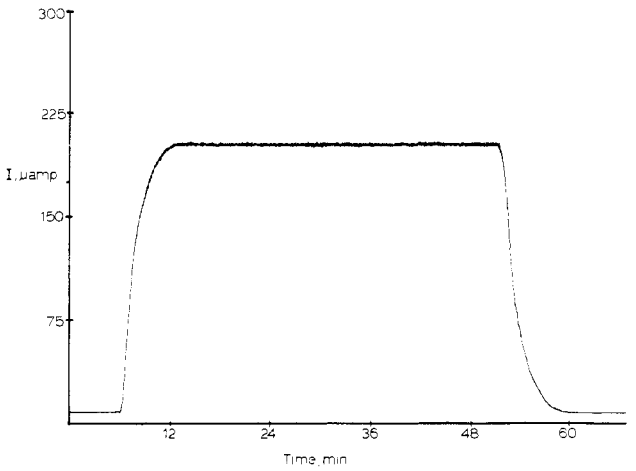

Figure 1. Current/time response for the H_2 cell. A typical photocurrent response curve is shown for the following conditions: $[Ru(bpy)_3^{2+}] = 5 \times 10^{-5}$ M, $[PQ^{2+}] = 2 \times 10^{-3}$ M, [TEOA] = 0.4 M, pH 9 in 0.1 M aqueous NaCl in the anode and 1.0 M HCl in the cathode. TEOA is triethanolamine. Both solutions were stirred at 300 ± 60 rpm and deaerated with Ar prior to photolysis at 436 nm.

ligible since the concentration of $Ru(bpy)_3^{2+}$ was relatively high (ϵ_{436} 1.25×10^4 M^{-1} cm^{-1}) and the steady-state concentration of PQ^+ was low as shown by spectral experiments on the cells at steady state.

In the case of the O_2 cell, the redox products $Co^{2+}(aq)$ and $H_2C_2O_4$ are transparent at 436 nm (note Scheme II). Thus, the A_Q term includes only the absorbance of $Co(Ox)_3^{3-}$ quencher (ϵ_{436} 182 ± 5 M^{-1} cm^{-1}) and the $Ru(bpy)_3^{3+}$ photoproduct. Because of the short photolysis times, any contribution from $Ru(bpy)_3^{3+}$ ($\epsilon_{436} \sim 1.6 \times 10^3$ M^{-1} cm^{-1}) is negligible compared to the sensitizer absorbance.

Note that although Φ_{cell} exhibits a specific wavelength dependence $\Phi_{intrinsic}$ is wavelength independent, and at sufficiently high sensitizer concentrations, the maximum efficiency is obtainable in the cells for broad-band irradiation throughout much of the visible. Cell efficiencies reported here have been corrected for absorbance losses and are therefore values of $\Phi_{intrinsic}$ unless states otherwise.

Under defined conditions in terms of incident light intensity and reactant concentrations, eq 13 can be written as in eq 16, with the term B in eq 16 being defined in eq 17. One point

$$q = B\phi_1\phi_2\phi_3 t = B\phi_1\phi_3 t\left(\frac{K_{sv}[Q]}{1 + K_{sv}[Q]}\right) \quad (16)$$

$$B = nFI^0_\lambda 10^{-A_s}(1 - 10^{-(A_{Ru}+A_Q)})\frac{A_{Ru}}{A_{Ru} + A_Q} \quad (17)$$

about these cells, which follows from eq 16 and 17, is that the constants B and ϕ_2 are calculable or measurable so that measurements of total charge as a function of time provide a means of evaluating such quantities as the separation efficiency, ϕ_3.

Equations 18 and 19 have been found to account for the

$$i = B\phi_1\phi_2\phi_3(1 + F\omega^m)(1 - \exp(-Gt)) \quad (18)$$

$$i = B\phi_1\phi_2\phi_3(1 - \exp(-Gt)) \quad (19)$$

current/time response for a related cell.[9] Equation 10 is applicable for a stirred-solution experiment and eq 19 for an experiment without stirring. ω is the stirring rate and m an empirical constant, which can be evaluated experimentally; F and G are constants characteristic of the cell. Since the question of stirring dependence of the photocurrent in excited-state PEC cells has been addressed previously[9] and because we are interested only in steady-state measurements here, we have made no attempts to evaluate the constants F, m, and G, for the cells described here. The determination of these constants would add little to our discussion, and since the values depend strongly on cell geometry, they are of little use in making comparisons between different cells. At sufficiently long photolysis times, the exponential terms in eq 18 and 19 go to zero and a limiting photocurrent, i_l, is reached (note Figure 1), giving eq 20 and 21.

$$i_l = B\phi_1\phi_2\phi_3(1 + F\omega^m) \quad (20)$$

$$i_l = B\phi_1\phi_2\phi_3 \quad (21)$$

(without stirring)

There is an additional complication in the H_2 cell. From Scheme I a competition exists between back electron transfer between PQ^+ and $Ru(bpy)_3^{3+}$ and capture of $Ru(bpy)_3^{3+}$ by the scavenger S. The efficiency of H_2 production is directly tied to the competition between PQ^+ and S because PQ^+ is the charge carrier for H_2 production. The competition leads to an additional term, ϕ_4, which appears in the photocurrent and photocharge equations. ϕ_4 is defined in eq 22. The

$$\phi_4 = k_6[S]/(k_5[PQ^+] + k_6[S]) \quad (22)$$

detailed form of eq 22 is complicated for the scavengers used here. All have pH dependences, and the deprotonated forms are expected to be more reactive toward $Ru(bpy)_3^{3+}$ so that k_6 and ϕ_4 are expected to be pH dependent. In addition, the photogenerated charge carrier PQ^+ appears in eq 22 with the result that ϕ_4 is also time dependent. At sufficiently long times $[PQ^+]$ must reach a steady state where its rate of photochemical appearance is balanced by its depletion at the electrode (note Scheme I), a condition that is met at the limiting current shown in Figure 1. In the limiting-current region, the photocurrent is given by eq 23. Including ϕ_4 in the quantum

$$i_l = B\phi_1\phi_2\phi_3\phi_4 = B\phi_1\phi_3\frac{K_{sv}[PQ^{2+}]}{1 + K_{sv}[PQ^{2+}]}\frac{k_6[S]}{k_5[PQ^+] + k_6[S]} \quad (23)$$

yield relationships in eq 14a, 14b, and 15 gives eq 24–26.

$$\Phi_{cell} = 10^{-A_s}(1 - 10^{-(A_{Ru}+A_Q)})\phi_1\phi_2\phi_3\phi_4 = \frac{q}{nFI^0_\lambda t} \quad (24)$$

$$\Phi_{intrinsic} = \phi_1\phi_2\phi_3\phi_4 \quad (25)$$

$$\Phi_{max} = \phi_3\phi_4 = \phi_3 \quad \text{(at high [S]; note eq 22)} \quad (26)$$

Photoelectrochemical Production of H_2. The photoelectrochemical cell used for the production of H_2 is shown in diagram A. The response of the cell is shown by the cur-

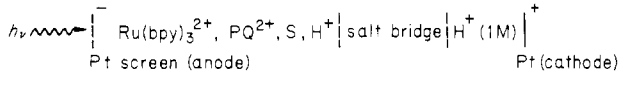

A

rent/time profile shown in Figure 1. In Figure 1 an initial exponential increase in current occurs as the concentration of PQ^+ builds up in the photolysis step, but with time the steady state is reached, and a limiting current appers in the cell. After the light is shut off, PQ^+ in the bulk of the solution continues to produce hydrogen and is depleted exponentially as it undergoes electron transfer at the electrode surface. The decay time for the dark current can be shortened significantly by stirring. It is important to note that, when information from the cell based on total charge passed is obtained, the total integrated area under both the photocurrent and the dark current must be used.

In order to test the mechanism proposed in Scheme I in terms of both the chemical reactions involved and the equations

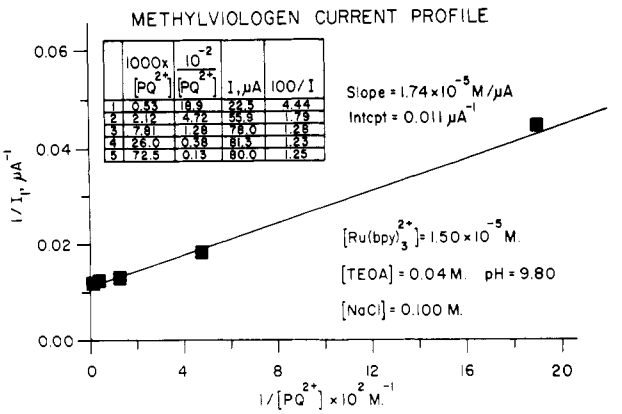

Figure 2. Variation of photocurrent with quencher concentration for the H_2 cell. The data shown are for the $Ru(bpy)_3^{2+}/PQ^{2+}$/TEOA cell and are seen to conform to the theoretical predictions of eq 27 in the text. The cathode contains 1.00 M H^+. Stirring speed is 200 ± 40 rpm.

describing the operation of the cell, we have carried out a series of experiments. The first experiment to mention is a verification of the stoichiometry suggested in Scheme I with regard to H_2 production. Following photolysis and measurement of the total charge in the cell, H_2 was collected quantitatively and analyzed by gas chromatography. The actual amount collected was found to agree within experimental error with that calculated from the total charge ($(3.9 \pm 0.2) \times 10^{-6}$ vs. $(4.1 \pm 0.2) \times 10^{-6}$ mol, respectively), showing that the reducing equivalents produced in the photoanode are transferred quantitatively to the second cell compartment.

The properties of the photocurrent were also investigated under a variety of conditions. A series of experiments was carried out to test the expected dependence of the limiting photocurrent on quencher concentration using a fixed concentration of triethanolamine (TEOA) as the scavenger. Equation 23, which describes the predicted dependence of i_l on both [S] and $[PQ^{2+}]$, can be rearranged to give eq 27 under

$$\frac{1}{i_l} = \frac{1}{B\phi_1\phi_3\phi_4 K_{sv}(1 + F\omega^m)} \frac{1}{[PQ^{2+}]} + \frac{1}{B\phi_1\phi_3\phi_4(1 + F\omega^m)} \quad (27)$$

conditions where [S] is held constant. The inverse relationship between i_l and $[PQ^{2+}]$ predicted by eq 27 is observed as shown in Figure 2. It is also expected from eq 27 that the intercept/slope ratio in Figure 2 is the Stern–Volmer constant, K_{sv}. The value $K_{sv} = 632 \pm 90$ M^{-1} calculated from Figure 2 is in good agreement with the value $K_{sv} = 651 \pm 50$ M^{-1} determined from luminescence quenching.

In a related series of experiments, the dependence of i_l on scavenger concentration, in this case EDTA, was also observed experimentally. For a constant quencher concentration where the photoelectrochemical steady state is reached and $[PQ^+]$ is constant, rearrangement of eq 23 gives eq 28. Once again, as shown in Figure 3, the theoretical prediction is in agreement with the experimental result.

$$\frac{1}{i_l} = \frac{k_5[PQ^+]}{B\phi_1\phi_2\phi_3 k_6(1 + F\omega^m)} \frac{1}{[S]} + \frac{1}{B\phi_1\phi_2\phi_3(1 + F\omega^m)} \quad (28)$$

The question of pH dependence of the cell with EDTA as scavenger is addressed by the data shown in Figure 4. In Figure 4 is shown a plot of i_l vs. pH at constant total [EDTA] and $[PQ^{2+}]$. The observed pH dependence is qualitatively consistent with an increased scavenging ability (i.e., the ability to undergo one-electron transfer) in the deprotonated forms of EDTA. The behavior exhibited here is in agreement with a recent study of the pH dependence of the reaction of $Ru(bpy)_3^{3+}$ with EDTA.[22] Both indicate that it is protonation of the EDTA that inhibits its reactivity with $Ru(bpy)_3^{3+}$ at pH 4. The oxidation is irreversible because of loss of a second electron and subsequent decomposition of the resulting amine.[22,23] In form, the current profile in Figure 4 describes a titration curve with an approximate $pK = 5.3 \pm 0.9$. Given the large number of species involved, all of which may have some reactivity toward $Ru(bpy)_3^{3+}$, and the several acid dissociation constants relating them, it is impractical to attempt

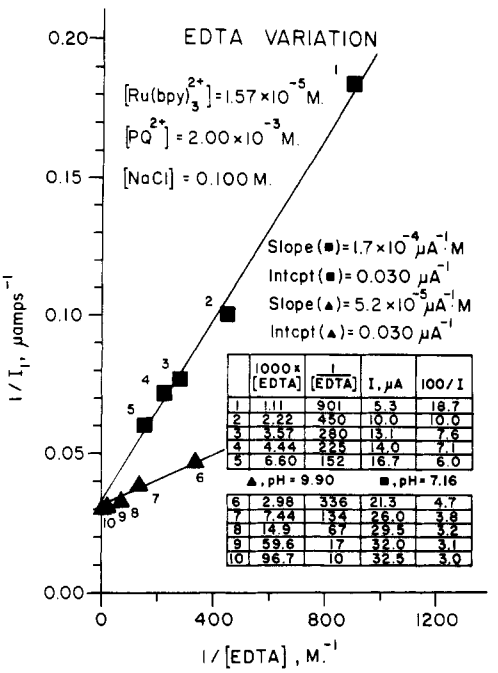

Figure 3. Relationship between photocurrent and scavenger concentration. The data for the $Ru(bpy)_3^{2+}/PQ^{2+}$/EDTA cell follow the relationship predicted by eq 28 at varying pH values. The intercept represents the theoretical current obtained for *complete* scavenging of $Ru(bpy)_3^{3+}$ by EDTA and, as expected, is independent of pH (note Scheme I). Stirring speed is 150 ± 30 rpm. Cathode solution is 1.0 M H^+.

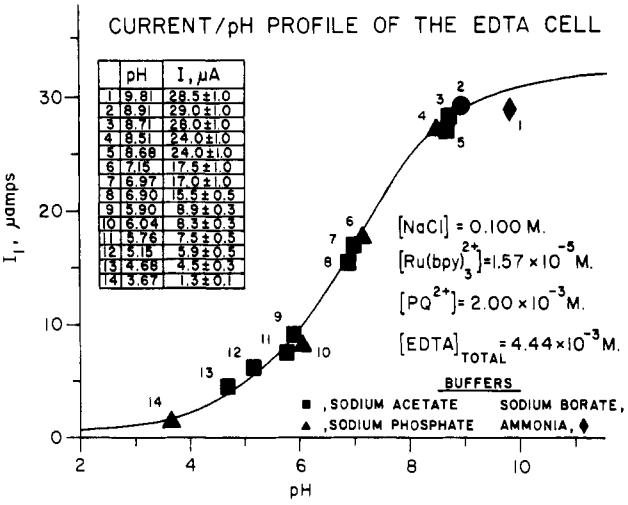

Figure 4. Effect of pH on the photocurrent in the H_2 cell. The shape of the curve for the $Ru(bpy)_3^{3+}/PQ^{2+}$/EDTA cell suggests that the deprotonated forms of EDTA are most active as scavengers for $Ru(bpy)_3^{3+}$ (note Scheme I). Note that the identity of the buffer used to maintain the solution pH does not affect the magnitude of the photocurrent. Other parameters are as in Figure 3.

(22) Miller, D.; McLendon, G. *Inorg. Chem.* **1981**, *20*, 950.
(23) Keller, P.; Moradpour, A.; Amouyal, E.; Kagen, H. *Nouv. J. Chim.* **1980**, *4*, 377.

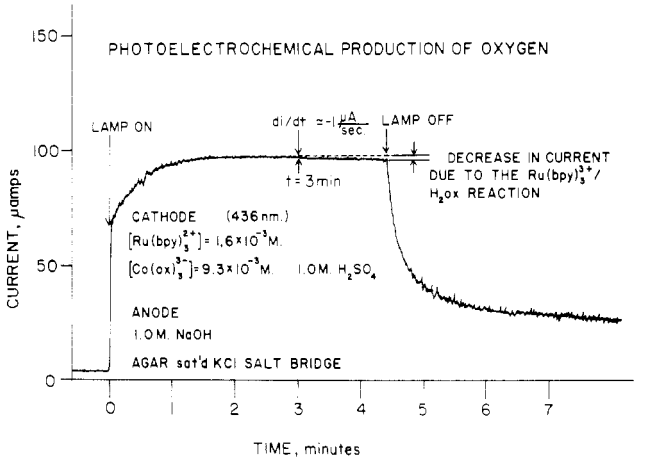

Figure 5. Photocurrent time dependence for the O_2 cell. Stirring speed is 200 ± 40 rpm. The decrease in photocurrent due to eq 29 is real and becomes increasingly more noticeable with extended photolysis times. Compare with Figure 1.

a detailed analysis of the curve in Figure 4.[24] However, the data make it quite clear that a pH dependence does exist and that a maximum scavenging efficiency is approached at high pH where the tetraanion ($EDTA^{4-}$) is the dominant form in solution.

Photoelectrochemical Production of O_2. The basic features of the photoelectrochemical O_2 cell are essentially the same as for the H_2 cell. An illustration is shown in diagram B. In

$$h\nu \rightsquigarrow \left| {}^{+} \right| Ru(bpy)_3^{2+}, Co(C_2O_4)_3^{3-}, H_2SO_4\,(1\,M) \left| \text{salt bridge} \right| OH^-\,(1\,M) \left| {}^{-} \right|$$

Pt screen (cathode) Pt (anode)

B

Figure 5 is shown a current vs. time plot for the cell. The basic features of the current/time response remain the same, including the initial exponential increase to a limiting value as predicted by eq 18. Once again, that the redox equivalents produced in the photo-half-cell, in this case functioning as a photocathode, are transferred quantitatively to the anode was verified by collecting the O_2 gas produced and analyzing it by gas chromatography ($(7.3 \pm 0.5) \times 10^{-6}$ mol calculated from the charge transferred through the cell vs. $(6.7 \pm 0.5) \times 10^{-6}$ mol by GC).

In contrast to the H_2 cell, where it was necessary to add a third component as a scavenger for $Ru(bpy)_3^{3+}$ following oxidative quenching, a back-reaction between separated redox products is avoided because of the irreversible loss of oxalate ligands from Co^{2+} in aqueous acid solution (note Scheme II). However, there is a complicating feature in the cell associated with the release of oxalic acid. Since oxalic acid reduces $Ru(bpy)_3^{3+}$ according to eq 29, there is a competition for

$$2Ru(bpy)_3^{3+} + H_2C_2O_4 \rightarrow 2Ru(bpy)_3^{2+} + 2CO_2 + 2H^+ \quad (29)$$

$Ru(bpy)_3^{3+}$ between $H_2C_2O_4$ and capture by electron transfer at the Pt electrode (note eq 11) in the cell. Since only that fraction of $Ru(bpy)_3^{3+}$ that reaches the Pt electrode is capable of producing a photocurrent, the photocurrent should fall with

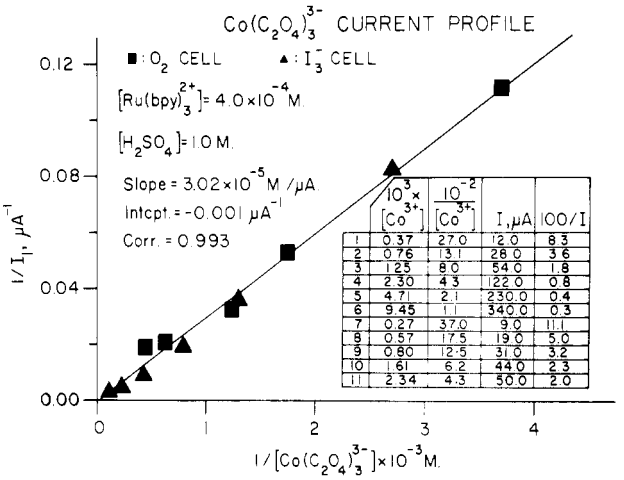

	$10^3 \times [Co^{3+}]$	$10^{-2}/[Co^{3+}]$	I, μA	100/I
1	0.37	27.0	12.0	8.3
2	0.76	13.1	28.0	3.6
3	1.25	8.0	54.0	1.8
4	2.30	4.3	122.0	0.8
5	4.71	2.1	230.0	0.4
6	9.45	1.1	340.0	0.3
7	0.27	37.0	9.0	11.1
8	0.57	17.5	19.0	5.0
9	0.80	12.5	31.0	3.2
10	1.61	6.2	44.0	2.3
11	2.34	4.3	50.0	2.0

Figure 6. Photocurrent variation with $[Co(C_2O_4)_3^{3-}]$: (▲) X = I^- cell; (■) X = OH^- cell. The relationship predicted by eq 35 is observed. Note that the identity of the species oxidized at the anode does not affect the results obtained. Stirring speed is 450 ± 80 rpm, and load resistance is 1000 Ω (1%).

time as oxalic acid is release. We have studied the kinetics of the reduction of $Ru(bpy)_3^{3+}$ by oxalic acid as described in the Experimental Section. From our data and eq 29 we derive the rate law given by eq 30. The values $K_1 = (5.5 \pm 0.4) \times 10^{-2}$ M and $K_2 = (1.58 \pm 0.01) \times 10^{-4}$ M represent the acid dissociation constants for oxalic acid[25] shown in eq 31 and 32.

$$\frac{-d[Ru(bpy)_3^{3+}]}{dt} = 2[Ru(bpy)_3^{3+}][H_2C_2O_4]\left(\frac{k_1K_1}{[H^+]} + \frac{k_2K_1K_2}{[H^+]^2}\right) \quad (30)$$

$$H_2C_2O_4 \overset{K_1}{\rightleftharpoons} HC_2O_4^- + H^+ \quad (31)$$

$$HC_2O_4^- \overset{K_2}{\rightleftharpoons} C_2O_4^{2-} + H^+ \quad (32)$$

At 23.0 ± 0.1 °C, we find that $k_1 = 5.66 \pm 0.85$ M^{-1} s^{-1} and $k_2 = (2.31 \pm 0.36) \times 10^4$ M^{-1} s^{-1} under these conditions. k_1 and k_2 represent the second-order rate constants for oxidation of $HC_2O_4^-$ and $C_2O_4^{2-}$, respectively. For the conditions used in the photoelectrochemical experiment, (1.0 M H_2SO_4, 23 ± 1 °C), the appropriate experimental rate constant is given by eq 33, and the half-time of the reaction when pseudo-first-order conditions are reached is then $t_{1/2} = 0.67[H_2C_2O_4]$ s.

$$k_{obsd} = 2\left(\frac{k_1K_1}{[H^+]} + \frac{k_2K_1K_2}{[H^+]^2}\right) = 1.03 \pm 0.21\ M^{-1}\ s^{-1} \quad (33)$$

Although the effect of the released oxalic acid could be accounted for quantitatively in the context of the theoretical model leading to eq 18 and 19, it is simpler to describe the effect qualitatively. From eq 33 and the reaction life-time, in the initial stages of photolysis the photocurrent will be unaffected because of the low levels of released oxalic acid. The current/time profile predicted by eq 18 is that observed initially (Figure 5). However, as shown in Figure 5, at increasing photolysis times the limiting current is not constant but decreases slowly. The origin of the decrease is in the increasingly competitive capture of $Ru(bpy)_3^{3+}$ by $H_2C_2O_4$ as the latter builds up during the photolysis.

(24) (a) In other studies,[24b,c] it has been demonstrated that in the related photooxidation of EDTA by certain organic excited states, the pH profiles obtained for the quantum yield (of photooxidation) are nearly identical with the i/pH profile for Figure 4. The suggestion that only the monoprotonated and totally deprotonated forms of EDTA are active as scavengers[24b] due to the presence of a non-hydrogen-bonded N site in these forms is consistent with our results and with the corresponding pK values[24c] (pK_a = 6.16 for $EDTAH_2^{2-}$ and pK_a = 10.22 for $EDTAH^{3-}$). (b) Bonneau, R.; Pereyre, J. *Photochem. Photobiol.* **1975**, *21*, 173. (c) Fife, D. J.; Moore, W. M. *Ibid.* **1979**, *29*, 43.

(25) Moorhead, E. G.; Sutin, N. *Inorg. Chem.* **1966**, *5*, 1866.
(26) Durham, B.; Meyer, T. J. *J. Am. Chem. Soc.* **1978**, *100*, 6286.

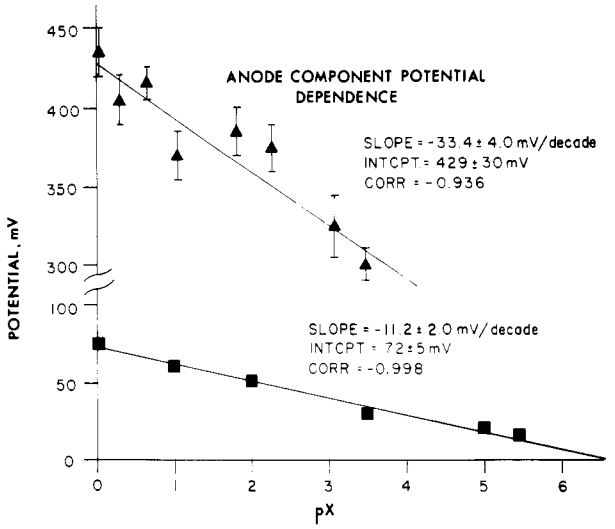

Figure 7. Photopotential measurements. The measurements were made with a 1000-Ω (1%) resistor as the load. Consult the text for an interpretation of the data. Data for both I^- (▲) and OH^- (■) cells are shown.

It should be noted that the complications associated with release of oxalic acid can be avoided by using $Co(NH_3)_5Cl^{2+}$ as the oxidative quencher in acid solution. With the chloropentaamminecobalt(III) ion as quencher, reduction to Co^{2+} gives NH_4^+ and Cl^- ions in solution and the $Ru(bpy)_3^{3+}$ ion is stable.[9]

For the O_2 cell, the quenching efficiency, ϕ_2, is given by eq 34. Using eq 34 in eq 18 for the limiting current and rearranging give eq 35, in which $\phi_1 \simeq 1$ is the efficiency of population[21] of $Ru(bpy)_3^{2+*}$ and ϕ_3 is the separation efficiency. As shown in Figure 6, the inverse/inverse dependence between i_l and $[Co(Ox)_3^{3-}]$ predicted by eq 35 is observed. The i_l values used in Figure 6 were taken from current/time plots early in the photolysis period before the release of oxalic acid was important.

$$\phi_2 = \frac{K_{sv}[Co(Ox)_3^{3-}]}{1 + K_{sv}[Co(Ox)_3^{3-}]} \tag{34}$$

$$\frac{1}{i_l} = \frac{1}{B\phi_1\phi_3K_{sv}(1 + F\omega^m)} \frac{1}{[Co(Ox)_3^{3-}]} + \frac{1}{B\phi_1\phi_3(1 + F\omega^m)} \tag{35}$$

Experiments were also carried out based on the oxidation of I^- to I_3^- in the anode. The reaction of $Ru(bpy)_3^{3+}$ with I^- is spontaneous as shown in eq 36, and as noted in Figure 6,

$$Ru(bpy)_3^{3+} + {}^3/_2I^- \rightarrow Ru(bpy)_3^{2+} + {}^1/_2I_3^- \qquad \Delta E = +0.73 \text{ V} \tag{36}$$

equivalent data are obtained for either I^- or OH^- in the anode compartment. With I^- present the anode reaction becomes eq 37. The variations of the operating cell potentials with

$${}^3/_2I^- \xrightarrow{Pt} {}^1/_2I_3^- + e^- \tag{37}$$

pOH and pI (pI = −log $[I^-]$) are shown in Figure 7. The measurements were made with use of a 1000-Ω (1%) resistor as the load. Linear relations were observed for both cells between cell potential and either pOH or pI. From the slopes of the two plots, the hydroxide ion dependence is 11 ± 2 mV/pOH unit in the O_2 cell and the iodide ion dependence is 33 ± 5 mV/unit for the I_3^- cell. These values are in reasonable agreement with values of 14.5 mV/decade and 29.5 mV/decade predicted from the Nernst equation for the half-cell reactions

$$4OH^- \rightarrow O_2 + 2H_2O + 4e^- \qquad I_3^- \rightarrow 3I^- + 2e^-$$

The measurement of the photopotential developed in the cell under near-potentiometric conditions ($i \leq 5$ nA with a potentiometer) gave a value of 0.81 ± 0.02 V for the O_2 cell and 0.69 ± 0.10 V for the I_3^- cell. The expected standard cell potentials are 0.86 and 0.72 V, respectively, on the basis of the half-cell potentials (measured vs. NHE)

$$Ru(bpy)_3^{3+} + e^- \rightarrow Ru(bpy)_3^{2+} \qquad E° = 1.26 \text{ V}$$

$$4OH^- \rightarrow 4e^- + 2H_2O + O_2 \qquad E° = -0.40 \text{ V}$$

$$3I^- \rightarrow I_3 + 2e^- \qquad E° = -0.54 \text{ V}$$

The agreement between the experimental and theoretical cell potentials is excellent, considering the fact that the cells were not run under standard conditions and contributions from concentration and overvoltage effects are included in the experimental measurements.

Conclusions

We have described here the design and operation of photoelectrochemical cells for the production of either H_2 or O_2. The cells are based on an initial excited-state electron-transfer quenching step in solution followed by diffusion of separated redox products to a collector electrode. Both of the cells are based on oxidative quenching:

$$Ru(bpy)_3^{2+*} + ox \rightarrow Ru(bpy)_3^{3+} + red \tag{38}$$

In one cell, the $Ru(bpy)_3^{3+}$ produced is scavenged by a third component, S, and PQ^+ is the electron-transfer carrier for producing H_2 in a second electrode compartment. In the second cell, the reduced quencher is "self-scavenged" by loss of ligands, giving $Co(H_2O)_6^{2+}$; $Ru(bpy)_3^{3+}$ becomes the electron-transfer carrier for either O_2 or I_3^- production. The *net reactions* occurring in these cells are, in the first case with cysteine as the example of the scavenger, the photocatalytic reduction of H^+ by cysteine

$$\underset{\text{anode}}{RS^-}\ (\text{pH } 8\text{–}10) + \underset{\text{cathode}}{H^+}\ (1\text{M}) \xrightarrow{h\nu} \underset{\text{anode}}{{}^1/_2RS\text{–}SR} + \underset{\text{cathode}}{{}^1/_2H_2} \tag{39}$$

and, in the second, the photocatalytic oxidtion of H_2O to O_2 by $Co(C_2O_4)_3^{3-}$:

$$\underset{\text{cathode}}{\{Co(C_2O_4)_3^{3-} + 6H^+\ (1\text{ M})\}} + \underset{\text{anode}}{OH^-\ (1\text{ M})} \xrightarrow{h\nu} \underset{\text{cathode}}{\{Co^{2+} + 3H_2C_2O_4\}} + \underset{\text{anode}}{\{{}^1/_4O_2 + {}^1/_2H_2O\}} \tag{40}$$

Neither of the cell reactions is especially notable in itself nor is there a suggestion that they may be practical in themselves. In that context the considerable pH gradients between the two cell compartments in both cells should be noted. However, the general concept of excited-state PEC cells and some of the possibilities for using them most certainly are worth noting, as suggested by the following comments.

(1) Excited-state PEC cells offer the advantage of applying the extensive and growing redox chemistry of molecular excited states in solution to a number of possible photoelectrochemical schemes.

(2) Excited-state PEC cells are potentially of value as measuring devices both for light intensities and for parameters that characterize the underlying homogeneous photochemistry.[9]

(3) Such cells deserve and are receiving serious consideration in energy conversion schemes.[3,4,27,28] Significant photocurrents

(27) Neumann-Spallart, M.; Kalayanasundaran, K.; Gratzel, C.; Grätzel, M. *Helv. Chim. Acta* **1980**, *63*, 1112.

can be obtained, and the chemical products produced by photolysis appear already separated in isolated cell compartments.

(4) In a comparison with semiconductor PEC cells there are a number of advantages. There are no complications or requirements arising from photolysis at an interface or from materials problems such as electrode photodecomposition. The electrode acts only as a "collector". The quantitative details of the cells are determined by homogeneous photochemical reactions, which can be studied with use of routine experimental techniques (e.g., luminescence quenching, quantum yield determination, and flash photolysis), and their current/voltage/time characteristics are derivable in a straightforward fashion.[9] It follows that the maximization of cell performance is a chemical problem solvable by synthesis and measurements in solution rather than a problem in solid-state physics.

(5) Specifically, when the problem of water splitting or other solar to chemical energy conversion schemes is dealt with, the cells may find direct application. Following either oxidative or reductive quenching, water must enter the scheme, probably in a catalyzed step, as either an oxidative or a reductive "scavenger". One example of a workable scheme based on $Ru(bpy)_3^{2+}$ is shown in Scheme III. It relies on initial oxidative quenching followed by the reduction of water by the reduced quencher. The reduction of water must be made to occur on a time scale that is short compared to back electron transfer between $Ru(bpy)_3^{3+}$ and red. The energy conversion cycle could be completed on a relatively leisurely time scale by electrochemical oxidation of H_2O by $Ru(bpy)_3^{3+}$ in a separate cell compartment. Given the relatively low intensity of the solar flux, the demands placed on electrodes in terms of current densities are far less than those associated with fuel cells.

Scheme III

$$Ru(bpy)_3^{2+} \xrightarrow{h\nu} Ru(bpy)_3^{2+*}$$

$$Ru(bpy)_3^{2+*} + ox \rightarrow Ru(bpy)_3^{3+} + red$$

$$red + H_2O \rightarrow ox + {}^1/_2H_2 + OH^-$$

$$Ru(bpy)_3^{3+} + e^- \xrightarrow{Pt} Ru(bpy)_3^{2+}$$

$$OH^- \xrightarrow{Pt} {}^1/_4O_2 + {}^1/_2H_2O + e^-$$

(6) The possibilities for developing other energy storage reactions based on excited-state PEC cells are clear.[26-29] It should be reemphasized that one of the real values of such cells is their basis in homogeneous photochemistry since further developments in that area will provide the basis for additional cells. The experimental bases for individual half-cells can be studied separately and combined later in a net cell.

Acknowledgments are made to the National Science Foundation for a fellowship for W.J.D., to the Chaim Weizmann Postdoctoral Fellowship Program for fellowship support for B.D., and to the Department of Energy under Grant No. DE-A505-78ER06034 for support of this research.

Registry No. H_2, 1333-74-0; O_2, 7782-44-7; $Ru(bpy)_3^{2+}$, 15158-62-0.

(28) Chandrasekaran, K.; Whitten, D. G. *J. Am. Chem. Soc.* **1980**, *102*, 5119.

(29) Sullivan, B. P.; Dressick, W. J.; Meyer, T. J. *J. Phys. Chem.* **1982**, *86*, 1473.

Contribution from Department of Chemistry, Texas A&M University, College Station, Texas 77843

Electronic Structure of Metal Clusters. 2. Photoelectron Spectrum and Molecular Orbital Calculations of Decacarbonyldihydridotriosmium

DAVID E. SHERWOOD, JR., and MICHAEL B. HALL*

Received December 3, 1981

Molecular orbital (MO) calculations and the gas-phase ultraviolet photoelectron (PE) spectrum are reported for $H_2Os_3(CO)_{10}$. In a comparsion with the PE spectrum of $Os_3(CO)_{12}$, the major spectral change is loss of a band due to a direct Os–Os bond and appearance of bands due to Os–H–Os bridge bonds. The spectrum also shows a substantial rearrangement of the bands due to the pseudo-t_{2g} electrons, which are usually considered Os–CO π bonding but Os–Os nonbonding. The molecular orbital results, which are described in terms of the pseudooctahedral fragments, $Os(CO)_4$ and $Os(CO)_3$, suggest that the rearrangement of the pseudo-t_{2g} electrons results in a partial Os–Os bond between the hydrogen-bridged osmiums. The calculations also suggest that donation into a low-lying Os–Os antibonding orbital is responsible for the increase in Os–Os bond distance as bridging hydrogens are replaced by bridging methoxide groups.

Introduction

There has been a great deal of interest in the chemistry, structure, and bonding of decacarbonylbis(μ-hydrido)-*triangulo*-triosmium, $(\mu\text{-}H)_2Os_3(CO)_{10}$, since it was first synthesized by Johnson, Lewis, and Kilty.[1] This complex undergoes oxidative addition with alkenes[2] and alkynes,[3] under much milder reaction conditions than the simple parent carbonyl species, dodecacarbonyl-*triangulo*-triosmium, $Os_3(CO)_{12}$. Two-electron-donor ligands, L (L = carbonyl, phenyl cyanide, or phosphines), can add associatively to $(\mu\text{-}H)_2Os_3(CO)_{10}$ to give $(\mu\text{-}H)_2Os_3(CO)_{10}(L)$ complexes, which, when heated, produce $(\mu\text{-}H)_2Os_3(CO)_9(L)$ species.[4] One or both bridging hydrides can be replaced by bridging alkoxides[1] or thiolates.[5] Both the oxidative addition and the associative addition reactions involve donation of ligand electrons to $(\mu\text{-}H_2)Os_3(CO)_{10}$. In comparison to the parent carbonyl, the hydrido species loses two carbonyl ligands, representing four cluster electrons, and gains one H_2 unit, representing two cluster

(1) Johnson, B. F. G.; Lewis, J.; Kilty, P. *J. Chem. Soc. A* **1968**, 2859.
(2) (a) Deeming, A. J.; Hasso, S. *J. Organomet. Chem.* **1976**, *114*, 313. (b) Deeming, A. J.; Hasso, S. *Ibid.* **1975**, *88*, C21. (c) Keister, J. B.; Shapley, J. R. *J. Am. Chem. Soc.* **1976**, *98*, 1056. (d) Bryan, E. G.; Johnson, B. F. G.; Lewis, J. *J. Organomet. Chem.* **1976**, *122*, 249.
(3) (a) Deeming, A. J.; Hasso, S.; Underhill, M. *J. Organomet. Chem.* **1974**, *80*, C53. (b) Jackson, W. G.; Johnson, B. F. G.; Kelland, J. W.; Lewis, J.; Schorpp, K. T. *Ibid.* **1975**, *87*, C27.
(4) Deeming, A. J.; Hasso, S. *J. Organomet. Chem.* **1975**, *88*, C21.
(5) See, for example: Allen, V. F.; Mason, R.; Hitchcock, P. B. *J. Organomet. Chem.* **1977**, *140*, 297-307.

0020-1669/82/1321-3458$01.25/0